

Ultrasonic Detection of Spall Damage Distribution Subjected to Plate Impact Test with Different Thickness

Naoya Nishimura^{1,*}, Toshihiro Ito², and Takeru Watanabe³

¹Meijo University, Department of Vehicle and Mechanical Engineering, 1-501 Shiogamaguchi, Tempaku-ku, Nagoya 468-8502, Japan

²Nagoya Institute of Technology, Department of Mechanical Engineering, Gokiso-cho, Showa-ku, 468-8555 Nagoya, Japan

³Oshima Collage, National Institute of Technology, 1-1091 Komatsu, Suo-Oshima, 742-2193 Oshima, Japan

Abstract. Plate impact test on medium carbon steel were carried out to the target plate by impacting the flyer plate with one-third and two-thirds thickness of the target plate. The spall damage within the target plate was evaluated non-destructively with a low frequency scanning acoustic microscope as well as ultrasonic velocity and backscattering intensity. We observed the spall damage distribution by the B- and C-scan images. The distribution of spall damage through the plate thickness depends on the tensile stress area within the target plate. The difference of spall damage distribution was investigated by the plate impact test by flyer plate with different thickness. In the plate impact test by the flyer plate with 1/3 target plate thickness, the spall damage was generated by tensile stress area which superposed in the back surface side. On the other hand, in the case of 2/3 target plate thickness, the spall damage was detected at the impact surface side. By generating the spall damage in the different position through the target thickness, it will be possible to evaluate the accumulation of spall damage by reflection and transmission of the stress wave at the internal damage subjected to repeated impact.

1 Introduction

Spall damages, microvoids or microcracks, are nucleated by intensive tensile stress pulse within a solid which has been impacted at high velocity. Spall damage is invisible, because it appears within a solid. Traditionally the extent of spall damage has been examined by destructive means, namely sectioning and polishing the sample and observation with an optical or scanning electron microscope [1-3]. However these destructive methods are applied to neither actual structural parts nor investigation of the spall damage growth by successive impacts on the identical sample.

For the non-destructive evaluation of the spall damage, we should know the size and the quantity of the minute damage as well as the location. Among many non-destructive methods, an ultrasonic method is versatile and suitable for quantitative evaluation. Namely, we can visualize minute defects within solids by C- and B-scan images, which give us defect distribution at an arbitrary depth in a plane parallel to the impacted plane and in a longitudinal cross section. In addition, with the conventional pulse-echo measurement, we can measure ultrasonic wave velocity, amplitude ratio of B2 to B1 echo and backscattering intensity from the defect. Thus, we can detect and evaluate non-destructively the spall damage within the material.

The aim of the present paper is to reveal with ultrasonic technique the difference of spall damage

distribution subjected to the plate impact test by flyer plate with different thickness, in order to evaluate the growth process of spall damage under repeated impact by reflection and transmission of the stress wave at the internal damage.

2 Spallation under plate impact test

Spall damage is nucleated within a target plate by triaxial tensile stress pulse which is generated by the plate impact test. Figure 1 shows the stress wave propagation after two plates have collided, under the assumption that both plates have the same mechanical properties and the target plate has double thickness of the flyer. When a target plate is impacted by a flyer plate at high velocity, at time t_1 , the compressive stress waves travel toward the free surfaces of both plates. The waves are reflected at the free surfaces with the reversed phase, namely tensile nature. Then, the reflected waves travel back toward the impacted surface with cancelling the compressive wave, as show at time t_2 . Thus it is called as rarefied wave. When both rarefied waves from the free surfaces are superposed, at time t_3 , the real tensile stress pulse is generated in the shaded domain. When the stress is higher than the spall threshold stress of the solid, the spall damage is nucleated there. The extent of the damage depends on the magnitude as well as duration of the tensile stress pulse. Thus, the damage grows within a

* Corresponding author: nisimura@meijo-u.ac.jp

thin layer, often called as the spall plane, in which the duration of tensile pulse is longest.

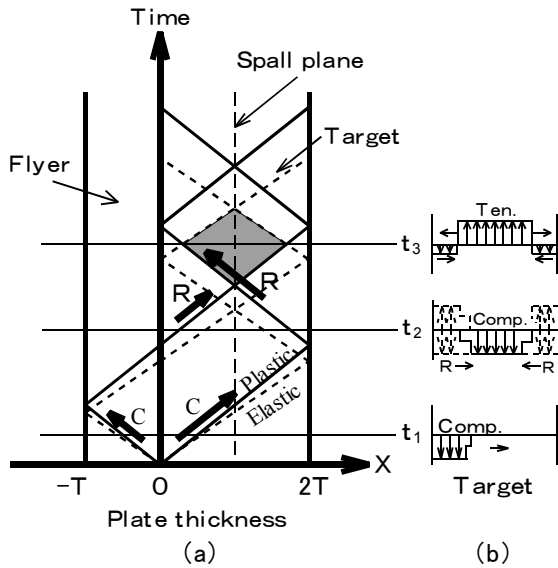


Fig. 1. (a) Stress wave propagation within target and flyer plates. (b) Stress distribution.

3 Experimental method

3.1 Plate impact test

Target plates made of medium carbon steel were impacted repeatedly by a flyer plate of the same material with a gas gun. The thickness of the flyer plate was one-third and two-thirds thickness of the target plate. Figure 2 shows the stress wave propagation in each flyer plate. The tensile stress pulse within the target plate impacted by the flyer plate with 1/3 and 2/3 target plate thickness appears in the back and impacted surface side, respectively. The dimensions of the target and the flyer plates are shown in Fig.3. In order to realize the uniaxial strain state in the target plate, the parallelism of the target and flyer plates should be less than 1mrad [4]. The flyer plate bonded to the plastic sabot was accelerated by a single stage gas gun. The target plate was also bonded the plastic holder which was fastened to the target holder and velocity measurement unit, as shown in Fig.3. The velocity of the flyer was measured by the optical fiber switches 20 and 30 mm away from the target plate.

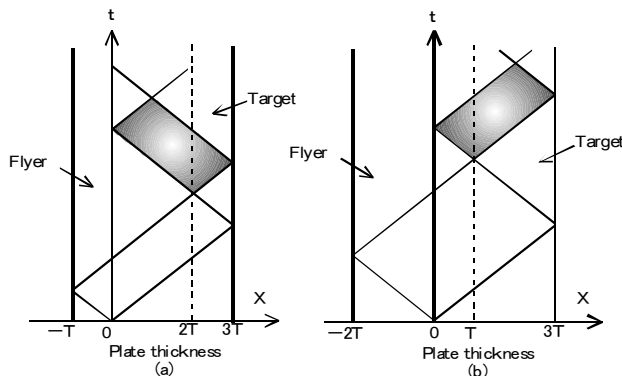


Fig. 2. Stress wave propagation (only elastic wave). Flyer plate thickness is (a) 1/3 and (b) 2/3 of target plate.

The compressive stress at the impacted surface is estimated by

$$\sigma = \frac{1}{2} \rho C V, \quad C = \sqrt{\frac{K}{\rho}} \quad (1)$$

where ρ , K and V are the density and bulk modulus of the material, and the velocity of the flyer.

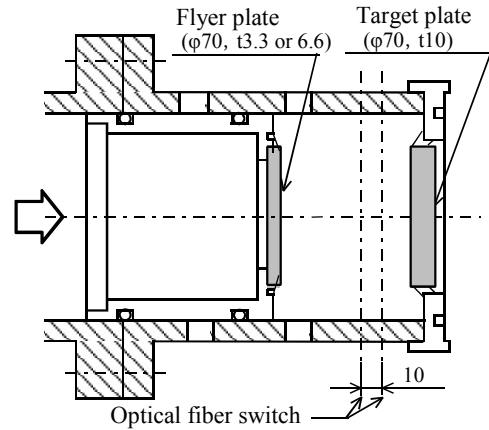


Fig. 3. Target, flyer and velocity measurement unit.

3.2 C- and B- scan imaging

The scanning acoustic microscope used in this study is Olympus UH Pulse-100. The block diagram is given in Fig.4. Spall damage distribution in the target plate was examined by ultrasonic C- or B-scan image which visualized the void or crack distribution in a plane parallel or perpendicular to the impact plane. The image is constructed with the amplitude of the longitudinal wave reflected at voids or cracks by scanning the focused ultra-sonic beam. The spatial resolution of the image depends on the beam diameter at the focus. We used a PVDF transducer of which central frequency, diameter and focal length are 30 MHz, 6.3 and 25.4 mm, respectively. The beam diameter at the focus is about 0.28 mm [5]. A PVDF transducer is free from the noise owing to the reverberation at the lens surface in the conventional transducer, therefore voids or cracks in arbitrary depth are imaged clearly.

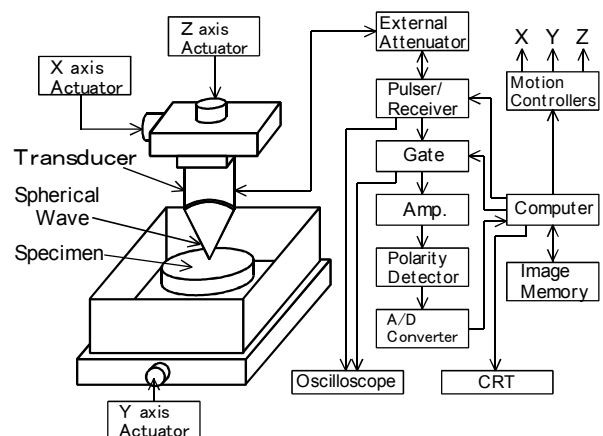


Fig. 4. Block diagram of acoustic microscope.

3.3 Quantitative evaluation of spall damage

For quantitative evaluation of the spall damage evolution, the time-of-flight (velocity) and the backscattering intensity scattered at the spall damage were measured with a digital ultrasonic measurement system [6], as shown in Fig.5. The measurement system is composed of an ultrasonic pulser/receiver, A/D converter board and personal computer. A longitudinal wave transducer was used, of which frequency and diameter were 10 MHz and 6.4 mm respectively. The waveform of the backwall echoes and the backscattering echo was recorded at three locations on the target plate. As an example, Figure 6 shows a received wave form on the impacted specimen, from which the ultrasonic velocity and amplitude ratio of B2 to B1 echo were calculated. The backscattering intensity depending on frequency is evaluated by the non-dimensional value,

$$N = \int_{f_1}^{f_2} B(f)df / \int_{f_1}^{f_2} U(f)df \quad (2)$$

where B(f) and U(f) are the amplitude spectrum of the backscattering wave and surface echo, and f1 and f2 are lower and upper limits of frequency range, namely 3 and 14 MHz. After the final ultrasonic measurement, the target plate was sectioned and the damage was observed by an optical microscope.

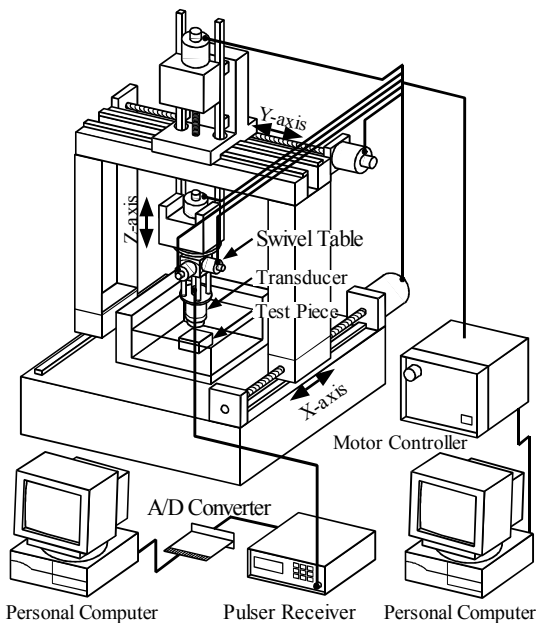


Fig. 5. Digital ultrasonic measurement system.

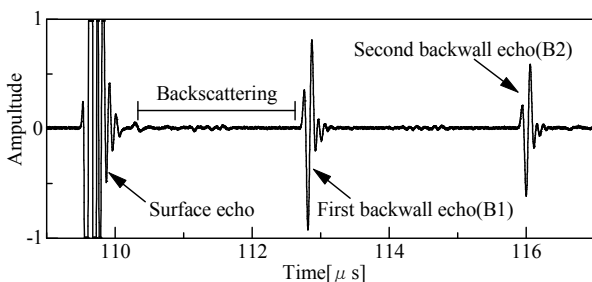


Fig. 6. Example of received waveform.

4 Experimental results

The velocity histories given to the target plates and estimated impact stresses are shown in Table 1. The spall threshold stress of medium carbon steel has estimated to be less than 2.4-2.6 GPa by damage detection with the acoustic microscope [7].

Table 1. Impact velocity and Estimated stress.

| Flyer : Target = 1 : 3 | | |
|------------------------|-----------------------|---------------------|
| Specimen No. | Impact velocity [m/s] | Impact stress [GPa] |
| U1 | 174 | 4.0 |
| U2 | 199 | 4.6 |
| U3 | 143 | 3.3 |
| U4 | 109 | 2.5 |
| U5 | 152 | 3.5 |
| U6 | 166 | 3.8 |

| Flyer : Target = 2 : 3 | | |
|------------------------|-----------------------|---------------------|
| Specimen No. | Impact velocity [m/s] | Impact stress [GPa] |
| M1 | 112 | 2.6 |
| M2 | 107 | 2.5 |
| M3 | 138 | 3.2 |
| M4 | 102 | 2.4 |
| M5 | 152 | 3.5 |

4.1. Spall damage distribution

Figures 7 and 8 show the C-scan images of the spall damage within the medium carbon steel after the plate impact test by the flyer plate with 1/3 and 2/3 target plate thickness. These images were taken at 3.0 mm depth from the impact or rear surface side of the target plate with the same imaging conditions. The gate width was fixed at 30 ns which corresponds to approximately 90 μm thickness in the steel we investigate. The white spots caused by reflected signal indicates the defects. In the plate impact tests, we applied different impact stresses to specimens (see the details in Table 1) in order to evaluate the damage distribution through the thickness. Thus these C-scan images show the spall damage distribution.

In Figure 7, the plate impact test by the flyer plate with 1/3 target plate thickness, the spall damage was generated in the back surface side. On the other hand, in the case of 2/3 target plate thickness (Figure 8), the spall damage was detected at the impact surface side. The distribution of spall damage through the plate thickness depends on the tensile stress area where the rarefied wave started the superposition first within the target plate (see Figure 2). And the density of the defects in specific spall damage zone increases with the impact stress.

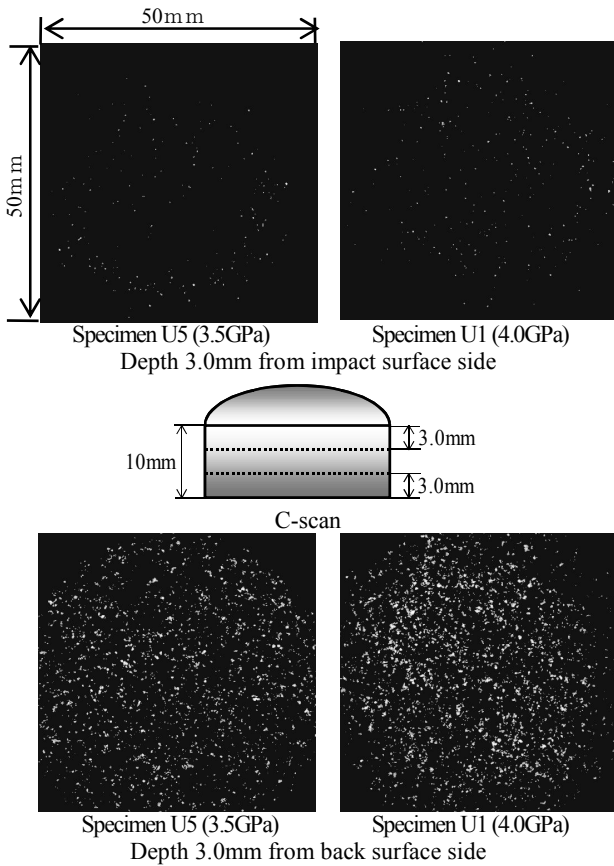


Fig. 7. Spall damage distribution by C-scan image. (Flyer: Target = 1 : 3).

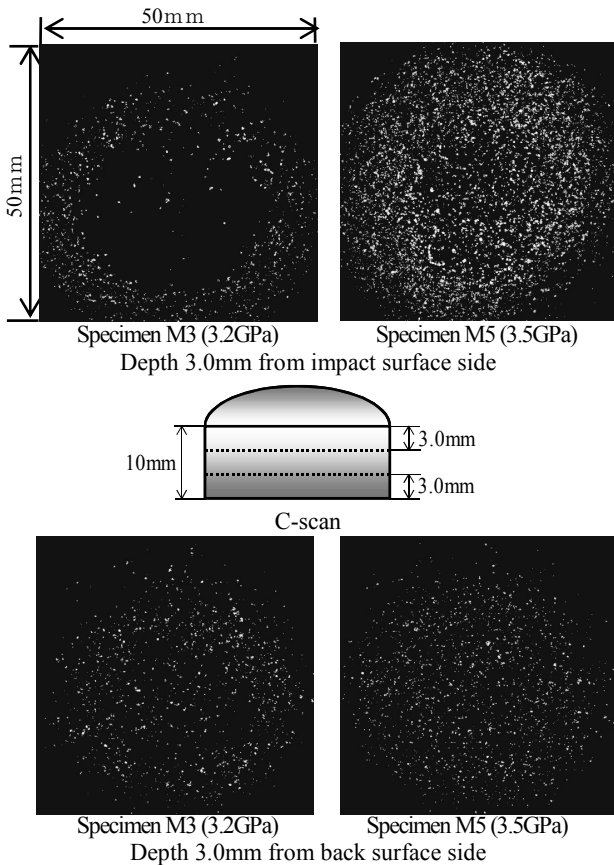
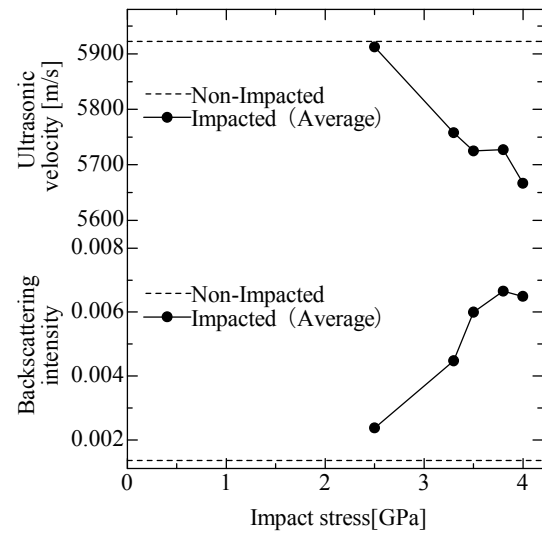


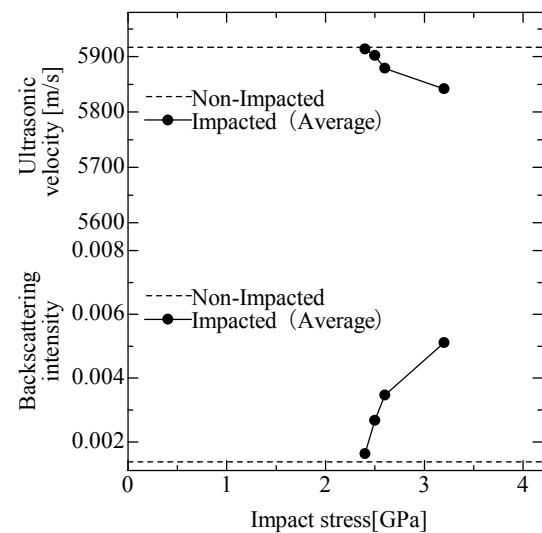
Fig. 8. Spall damage distribution by C-scan image. (Flyer: Target = 2 : 3).

4.2 Change in ultrasonic velocities and backscattering intensity

When a solid includes a lot of voids or cracks, the wave velocity has decreased but the backscattering intensity has increased due to the ultrasonic wave scattering at voids or cracks. Thus the spall damage extent is correlated with ultrasonic wave velocity and backscattering intensity. The longitudinal wave velocity and backscattering intensity are shown in Figure 9 for the each impact stress. When the impact stress is lower than the spall threshold stress (approximately 2.5 GPa), the ultrasonic velocity is equal to that of non-impacted plates, and the backscattering intensity are also unchanged. It is clear that the higher the impact stress, the lower the velocity. The backscattering intensity increases with impact stress. Thus, these ultrasonic variables characterize the spall damage quantitatively.



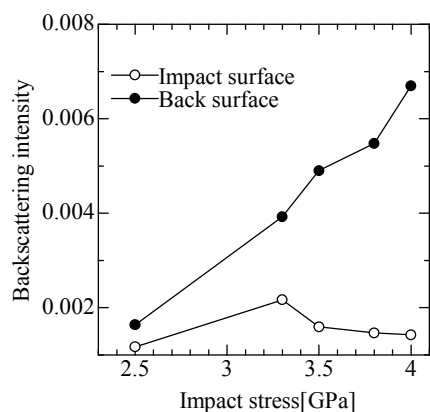
(a) Flyer:Target=1:3



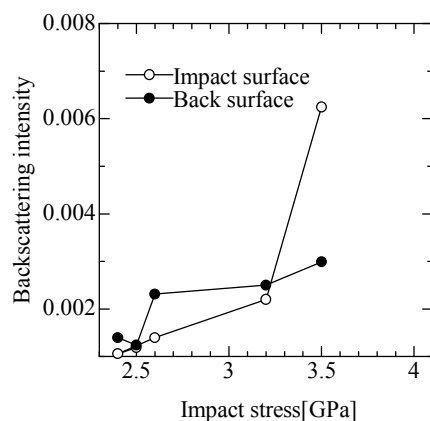
(b) Flyer:Target=2:3

Fig. 9. Change in ultrasonic velocity and backscattering intensity on impact stress. Flyer plate thickness is (a) 1/3 and (b) 2/3 target plate.

On the ultrasonic measurement, the waveform which was measured from impacted and back surface was recorded and investigated. Figure 10 shows the backscattering intensity at approximately 3.0mm depth from each surface. In the specimen which was impacted by the flyer with 1/3 (Figure 10(a)) and 2/3 target plate thickness (Figure 10(b)), the backscattering intensity take higher value at the back and impact surface side, respectively. The change in C-scan image of the spall damage is well correlated with the change in backscattering intensity. Thus, these ultrasonic methods are useful to evaluate non-destructively the spall damage distribution.



(a) Flyer:Target=1:3



(b) Flyer:Target=2:3

Fig. 10. Dependence of backscattering intensity on impact stress. Flyer plate thickness is (a) 1/3 and (b) 2/3 target plate.

5 Conclusions

The change in the spall damage of medium carbon steel specimen, which was impacted by the flyer plate with 1/3 and 2/3 thickness of the target plate, was non-destructively evaluated with the ultrasonic C-scan images as well as the ultrasonic velocity and the backscattering intensity. The spall damage distribution through the plate thickness depended on the flyer plate thickness, i.e. the tensile stress area within the target plate. In the plate impact test by the flyer plate with 1/3 and 2/3 target plate thickness, the spall damage was nucleated at the back and impacted surface side, respectively. The change in C-scan images is well correlated with the change in these ultrasonic parameters. By generating the spall damage in the different position through the target thickness, it will be possible to evaluate the accumulation of spall damage by reflection and transmission of the stress wave at the internal damage subjected to repeated impact.

References

1. L. Davison, R. A. Graham, *Phys. Rep.*, **55**, 255-379 (1979)
2. M. S. Mayers, C. T. Aimone, *Progress in Mat. Sci.*, **2**, 1-96 (1983)
3. D. R. Curran, L. Seaman, D. A. Shockey, *Phys. Rep.*, **147**, 253-388 (1987)
4. Y. Oved, G. E. Luttwak, *J.Comp.Mat.*, **12**, 84 (1978)
5. G. S. Kino, *Acoustic Waves: Devices, Imaging, and Analog Signal Processing*, Prentice-Hall, 182 (1987)
6. K. Kawashima, I. Fujii, *Rev. Prog. in QNDE*, **14**, 203-209 (1995)
7. N. Nishimura, K. Kawashima, O. Nakayama, M. Kondo, *Trans. JSME-A*, **66**-643, 626-633 (2000)

